© 2017. Published by The Company of Biologists Ltd | Journal of Experimental Biology (2017) 220, 3802-3811 doi:10.1242/jeb.158287

RESEARCH ARTICLE

High diving metabolic rate indicated by high-speed transit to depth in negatively buoyant long-finned pilot whales

Kagari Aoki[1,2,*], Katsufumi Sato[2], Saana Isojunno[1], Tomoko Narazaki[2] and Patrick J. O. Miller[1]

ABSTRACT

To maximize foraging duration at depth, diving mammals are expected to use the lowest cost optimal speed during descent and ascent transit and to minimize the cost of transport by achieving neutral buoyancy. Here, we outfitted 18 deep-diving long-finned pilot whales with multi-sensor data loggers and found indications that their diving strategy is associated with higher costs than those of other deep-diving toothed whales. Theoretical models predict that optimal speed is proportional to (basal metabolic rate/drag)$^{1/3}$ and therefore to body mass$^{0.05}$. The transit speed of tagged animals (2.7±0.3 m s^{-1}) was substantially higher than the optimal speed predicted from body mass (1.4–1.7 m s^{-1}). According to the theoretical models, this choice of high transit speed, given a similar drag coefficient (median, 0.0035) to that in other cetaceans, indicated greater basal metabolic costs during diving than for other cetaceans. This could explain the comparatively short duration (8.9±1.5 min) of their deep dives (maximum depth, 444±85 m). Hydrodynamic gliding models indicated negative buoyancy of tissue body density (1038.8± 1.6 kg m^{-3}, ±95% credible interval, CI) and similar diving gas volume (34.6±0.6 ml kg^{-1}, ±95% CI) to those in other deep-diving toothed whales. High diving metabolic rate and costly negative buoyancy imply a 'spend more, gain more' strategy of long-finned pilot whales, differing from that in other deep-diving toothed whales, which limits the costs of locomotion during foraging. We also found that net buoyancy affected the optimal speed: high transit speeds gradually decreased during ascent as the whales approached neutral buoyancy owing to gas expansion.

KEY WORDS: Swimming kinematics, Body condition, Cetacean, Deep-diving marine mammals, Foraging strategy, *Globicephala melas*

INTRODUCTION

For breath-hold divers that feed at depth and replenish their oxygen stores at the surface, it is crucial to adopt strategies that minimize oxygen consumption and therefore maximize foraging time at depth. Various morphological, physiological and behavioural factors affect oxygen consumption. For example, diving responses such as a reduction in heart rate and peripheral vasoconstriction are remarkable in aquatic mammals and minimize the rate of oxygen consumption via the regulation of metabolic rate (Panneton, 2013). Cetaceans have evolved streamlined body shapes that reduce drag and a high aspect ratio of flukes that increases swimming efficiency (Fish and Rohr, 1999). These traits are thought to be acquired as adaptations to aquatic life. Even on a short time scale, they might regulate swimming patterns and buoyancy to reduce the rate of oxygen consumption.

Buoyancy is one of the primary external forces acting on aquatic animals and is reflected by the overall body density (ρ_{animal}). Marine mammals have substantial amounts of blubber, and ρ_{animal} is mainly determined by the relative amount of blubber (containing lipid) to lean tissue. While lean tissue is denser than water, lipid tissue is less dense, and animals with a large proportion of lipid will therefore have lower ρ_{animal} and be more buoyant (Beck et al., 2000; Biuw et al., 2003).

Buoyancy has been shown to influence the stroking patterns of swimmers, with increased gliding when buoyancy aids movement (Skrovan et al., 1999; Williams et al., 2000; Miller et al., 2004a). For example, fatter and more buoyant seals predominantly showed stroke-and-glide swimming on descent and ascent, and leaner and negatively buoyant seals were gliding throughout most of the descent phase (Sato et al., 2003). Buoyancy also affects the round trip locomotion cost to transit to depth (Miller et al., 2012). A recent study indicates that neutral buoyancy is the most efficient at minimizing locomotion cost (Sato et al., 2013).

Another key determination of the cost of locomotion is swim speed. The rate of oxygen consumption during stroking increases rapidly with speed because drag resistance scales quadratically with swim speed (Hind and Gurney, 1997); therefore, how animals choose their swim speed is crucial to understanding their energy budget. A key concept in animal locomotion and energetics is the cost of transport (COT, the metabolic energy required to transport the animal's mass over a unit distance; Schmidt-Nielsen, 1972; Videler and Nolet, 1990; Williams, 1999). To maximize the amount of oxygen (and hence duration) that can be used for foraging at depth, diving animals are expected to descend and/or ascend at an optimal swim speed that minimizes COT during propulsive swimming (Thompson et al., 1993; Gallon et al., 2007). A theory based on the external work of moving the body through water predicts that optimal swim speed increases with mass$^{0.05}$ (Sato et al., 2010), closely matching empirical allometric relationships between swim speed and body mass ranging from 0.5 kg seabirds to 90,000 kg blue whales, which showed that transit swim speed gradually increases with body mass$^{0.09\ (0.04–0.14)}$ (Watanabe et al., 2011).

Two biomechanical models have been used to explain optimal swim speed: the external work model and the actuator disc model. The external work model calculates the COT based on power (where power is buoyancy and drag force acting on swimming animals multiplied by the animals' speed) (Sato et al., 2010; Watanabe et al., 2011). The COT increases with deviation from neutral buoyancy when animals move in the direction hindered by buoyancy, but the optimal swim speed is predicted to remain unchanged despite deviations from neutral buoyancy. In other words, the external work

[1]Sea Mammal Research Unit, University of St Andrews, St Andrews, Fife KY16 8LB, UK. [2]Department of Marine Bioscience, Atmosphere and Ocean Research Institute, The University of Tokyo, 5-1-5 Kashiwanoha, Kashiwa, Chiba 277-8564, Japan.

*Author for correspondence (aokikagari@gmail.com)

K.A., 0000-0002-5986-9849

Received 28 February 2017; Accepted 10 August 2017

Journal of Experimental Biology

Journal of Experimental Biology (2017) 220, 3802-3811 doi:10.1242/jeb.158287

List of symbols and abbreviations

a	acceleration, change in speed (m s^{-2})
ADL	aerobic dive limit
AIC	Akaike's information criterion
ARTS	aerial rocket transmitting system (tagging system)
C_d	drag coefficient (unitless)
COT	cost of transport (the energy expenditure per distance travelled)
CI	credible interval
d	depth (m)
DIC	deviance information criterion
F_B	buoyancy (N)
F_D	drag (N)
g	acceleration due to gravity (9.8 m s^{-2})
L	body length (cm)
m	body mass (kg)
p	pitch angle (radians)
r	compressibility (proportion)
S	surface area (m^2)
U	speed (m s^{-1})
V_{air}	volume of air carried by the animal at the surface (m^3)
ρ_{air}	density of gas (kg m^{-3})
ρ_{animal}	overall body density of animal (kg m^{-3})
ρ_{sw}	density of seawater (kg m^{-3})
ρ_{tissue}	density of non-gas component of animal body (kg m^{-3})

model predicts that optimal swim speed is not affected by either buoyancy or pitch angle, but is affected by the basal metabolic rate and drag of animals (Sato et al., 2010). These predictions were supported by experiments on captive sea lions (Suzuki et al., 2014). The actuator disc model estimates the power consumed in order to counter gravity and drag forces. The actuator disc theory has been widely used in studies of flying animals and helicopters (Weis-Fogh, 1972; Ellington, 1984; Wakeling and Ellington, 1997). The model predicts that optimal speed is positively related to basal metabolic rate and increases slightly with deviations from neutral buoyancy (Miller et al., 2012).

Deep-diving animals are predicted to benefit from transiting to and from depth at the optimal speed and having neutral buoyancy, because this strategy maximizes the amount of oxygen available for efficient aerobic metabolism at depth. Indeed, tissue body density of sperm whales and northern bottlenose whales that employ steady swimming during dives is close to neutral buoyancy (Miller et al., 2004a, 2016). In contrast, short-finned pilot whales make relatively short dives and perform sprints reaching 4–9 m s^{-1}, possibly to chase prey, at the deepest portion of the dive (Aguilar Soto et al., 2008). We expect that pilot whales might have a different diving strategy in order to exploit a niche distinct from that of other deep divers.

Long-finned pilot whales *Globicephala melas* in the North Atlantic (Buckland et al., 1993) feed mainly on squid and other prey usually found in mesopelagic water (Desportes and Mouritsen, 1993). Animal-borne time–depth recorders revealed that long-finned pilot whales dive to depths of 300–600 m (Baird et al., 2002; Heide-Jørgensen et al., 2002). The whales spent more than half their time near the sea surface, during which they did not conduct dives. Little has been reported about their swimming kinematics during dives.

We used animal-borne recorders on free-ranging long-finned pilot whales in the coastal area of Norway and investigated the characteristics of their swimming kinematics (cruising speed and drag coefficient) and the buoyancy (i.e. tissue body density and diving air volume) in order to access their diving cost. We found high-speed transits to depth and negative buoyancy of tagged whales, which indicate a high-cost diving strategy differing from that in other deep-diving toothed whales that conserve energy spent on locomotion during foraging dives. We also evaluated any effect of buoyancy on the optimal transit speed.

MATERIALS AND METHODS

All research activities were performed under permits issued by the Norwegian Animal Research Authority (permit no., S2011/38782), in compliance with ethical and local use of animals in experimentation. The research protocol was approved by the University of St Andrews Animal Welfare and Ethics Committee and Woods Hole Oceanographic Institution's Animal Care and Use Committee.

Data collection

Field studies were conducted using the research vessel M/S Strønstad (29 m, engine driven) in the Vestfjord basin off Lofoten, Norway. This study was conducted during May and June in 2008–2010 and 2013. Non-invasive suction-cup tags were attached to individuals by using either a 5 m hand-pole or a pneumatic launching system (Aerial Rocket Transmitter System, ARTS; Kleivane, 1998), which has a greater effective tagging range up to 12–15 m. Tagging was conducted from a small motor boat (<10 m), usually deployed from a larger engine-driven research vessel (M/S Strønstad or H. U. Sverdrup II).

Animal-borne recorders

Two types of animal-borne recorders were used: W2000-PD3GT acceleration and speed data-loggers (diameter: 23 mm, length: 123 mm, mass: 90 g in air; Little Leonardo Co., Tokyo, Japan) and sound and movement recording DTAGs (Woods Hole Oceanographic Institution, MA, USA). The PD3GT logger recorded depth, water temperature and speed from a flywheel at 1 s intervals and 3-axis acceleration at 16 Hz. The version-2 DTAGs measured pressure, water temperature and 3-axis acceleration at 50 Hz, which was later downsampled to 5 Hz.

Tag-data analysis

Diving data were analysed using software IGOR Pro (Wave-Metrics Inc., Lake Oswego, OR, USA) and MATLAB (MathWorks Inc., Natick, MA, USA). The start and end of dives were defined as the time when the whales descended below and ascended above a depth of 2 m, respectively. All dives (maximum depth: ≥20 m) were divided into three phases: (1) the descent phase (from the start of the dive to the time when the whale's pitch first exceeded 0 deg, i.e. when it was no longer oriented downward); (2) the ascent phase [from the last time when an animal's pitch was downward (<0 deg) to the end of the dive]; and (3) the bottom phase (the time between the end of the descent phase and the beginning of the ascent phase). Dive depth was defined as the maximum depth of the dive. Acceleration in the tri-axis (longitudinal, lateral and dorso-ventral axes) directions can be divided into components related to the body orientation of the animal with respect to gravity (gravity-based components) and propulsive activities imposed by fluke thrust (specific components; Sato et al., 2003). Lower frequency (mostly gravity-based) acceleration of the longitudinal axis was used to calculate the pitch of a whale (Sato et al., 2003). Higher frequency specific acceleration of the dorso-ventral axis was used to identify stroking (i.e. fluking movements; Sato et al., 2003; for details, see also Aoki et al., 2012). According to power spectral density of the dorso-ventral axis (Sato et al., 2007), stroking was determined when oscillation on the dorso-ventral axis of the accelerometer exceeded a threshold that was set manually for each deployment (0.24–0.78 m s^{-2}). As the

Journal of Experimental Biology (2017) 220, 3802-3811 doi:10.1242/jeb.158287

accelerometer was not attached exactly parallel to the axes of the whale, we corrected possible off-axis placement on the body, following Johnson and Tyack (2003). Speed through the water was measured using an external propeller on the PD3GT logger. The propeller rotation count was converted to actual swimming speed (m s^{-1}) by using a calibration line obtained from a linear regression of rotation rate against swim speed (m s^{-1}), which was calculated from the rate of vertical depth change divided by the sine of the pitch (Sato et al., 2003) when sine |pitch|≥0.95. The coefficient of determination (r^2) from the linear regressions ranged from 0.92 to 0.97, and speed resolution was 0.017–0.019 m s^{-1}. The DTAG lacks a speed sensor; therefore, speed was estimated using the depth change rate divided by the sine of pitch, when |pitch|≥45 deg.

Using the international equation of state of seawater (UNESCO, 1981), the density of seawater was estimated at 1 s intervals using depth (m) and temperature (°C) measurements obtained using data loggers, with a fixed salinity estimate of 34.84‰ (Vogel, 1994). Water temperature ranged from 5.4 to 17.0°C, and the corresponding density of the seawater ranged between 1026.7 and 1029.8 kg m^{-3}.

Calculation of drag coefficient (C_d)

Drag was calculated from the deceleration rate during horizontal gliding: $F_D=ma$, where F_D is drag (N), m is body mass (kg) and a is acceleration (m s^{-2}; Feldkamp, 1987; Watanabe et al., 2006; Aoki et al., 2011). Therefore, C_d is given as:

$$C_d = 2 \cdot m \cdot (U_t - U_{t+1})/(\rho_{sw} S U^2), \quad (1)$$

where speed U at time t and at time t+1 (U_t and U_{t+1}) were averaged to yield the mean glide speed (U, m s^{-1}), seawater density ρ_{sw} (kg m^{-3}) was also averaged during these periods, and S is the total surface area of the animal (m^2). We extracted deceleration phases for two whales tagged with the PD3GT speed data logger when they swam horizontally (i.e. depth changes were zero) by using stroke-and-glide patterns. We estimated C_d in the depth range 15–556.5 m.

Estimation of body mass and surface area

Estimation of C_d requires values for the body mass (m) and surface area (S) of whales (Eqn 1). We obtained frame images of tagged whales by using a digital camera to estimate these values. To ensure that a tagged whale was oriented broadside to the digital camera, we obtained measurements of multiple photographs.

The number of pixels on the height of the dorsal fin was measured, and this measurement was converted to centimetres based on the length of the DTAG or PD3GT as a scale. Body length was estimated using Bloch's equation. The height of the dorsal fin is 7% of body length and was found to be constant regardless of body length, based on data for 301 male and 432 female pilot whales (Bloch et al., 1993). Whale body length was subsequently converted to an estimate of whale mass by using Lockyer's equation (m=0.00023$L^{2.501}$ for long-finned pilot whales), where L is body length (cm), which was a good fit for animals ranging in size from about 1.5 to 6.0 m in length (Lockyer, 1993). Surface area of the tagged whales was estimated as (S=0.018L–2.14, r^2=0.78), based on Bose and Curren's measurement (Bose et al., 1990; Curren, 1992) of the surface area of seven whales of Delphinidae ranging from 1.4 to 3 m in length.

Hydrodynamic glide model

During glides, acceleration along the swimming path was determined as the difference between drag (F_D) and buoyancy (F_B) parallel to the swimming path: $ma=F_B\sin(p)-F_D$ (Miller et al., 2004a). Therefore, acceleration is given as (Miller et al., 2016):

$$a = -0.5 \cdot \frac{C_d S}{m} \cdot \rho_{sw} \cdot U^2 + \left(\frac{\rho_{sw}}{\rho_{tissue}(d)} - 1\right) \cdot \boldsymbol{g} \cdot \sin(p) + \frac{V_{air}}{m} \cdot \boldsymbol{g} \cdot \sin(p) \cdot \frac{\rho_{sw} - \rho_{air} \cdot (1 + 0.1d)}{(1 + 0.1d)}, \quad (2)$$

where

$$\rho_{tissue}(d) = \frac{\rho_{tissue}(0)}{1 - r \cdot (1 + 0.1d) \cdot 101,325 \times 10^{-9}}. \quad (3)$$

Here, ρ_{tissue} is the density of the non-gas component of the whale body (kg m^{-3}), $\boldsymbol{g}$ is the gravitational acceleration (9.8 m s^{-2}), p is animal pitch (radians), V_{air} is the volume of air carried by the whale at the surface (m^3), ρ_{air} is the density of air (kg m^{-3}), d is glide depth (m) and r is compressibility for an animal tissue or the fractional change in volume per unit increase in pressure. The value 101,325 converts pressure in atmospheres to pressure in Pascals, so that the units of body tissue compressibility are proportion $\times10^{-9}$ Pa^{-1}.

The model consists of three terms that estimate external forces acting on gliding whales: the first term is drag, the second term is buoyancy derived from the density of the non-gas component of the whale body, and the third term is buoyancy derived from the residual air carried by the animal (see Miller et al., 2016, for more detailed explanation of the equation).

Bayesian estimation of tissue body density and diving gas volume

Gliding data were extracted for 5 s-duration segments during dives following Miller et al. (2016). Acceleration during glides (a) was measured using a linear regression line of speed versus time. Standard error of acceleration for each 5 s segment was used to calculate the observation error, which was incorporated in the model by treating acceleration as a normal variable with a precision parameter (1/variance) that could vary from one glide segment to the next (Miller et al., 2016). We added a small increment (0.001) to the standard errors to ensure finite values for the precision parameter. Pitch (p), sea water density (ρ_{sw}) and speed (U) were averaged during each glide period. Only stable glides (circular variance of roll, pitch and head <0.1; correlation coefficient of acceleration slope >0.3) during descent and ascent phases when absolute pitch was steeper than 30 deg were included in the analysis. To estimate the body density of tagged whales, we used 14 individuals that had more than both five deep (>100 m) and five shallow (<100 m) glides. The model predicts that shallow glides (<100 m) are affected by both residual air and tissue body density, but deep glides are mainly affected by tissue body density owing to the compression of air following Boyle's law. Therefore, we require both deep and shallow glides to estimate the tissue body density and residual air of animals.

We used a Bayesian statistical procedure to estimate tissue body density, diving gas volume and drag following methods described in Miller et al. (2016). There are three unknown terms in the equation, each of which was set to a specific prior range. Body tissue density (ρ_{tissue}) was set at a uniform prior from 800 to 1200 kg m^{-3}, and diving gas volume was set at a uniform prior from 5 to 80 ml kg^{-1}. We calculated the drag term C_dS/m by using horizontal glides (Eqn 1) from two whales tagged with the PD3GT, which we could use to set the prior even without specific information on body mass and reference surface area. The mean (24.0×10^{-6} m^2 kg^{-1}) and standard deviation (3.0×10^{-6} m^2 kg^{-1}) of the normal prior were set at the median and quartile values of the drag terms calculated from

Journal of Experimental Biology (2017) 220, 3802-3811 doi:10.1242/jeb.158287

the horizontal glides. Data that were used to calculate the drag term were not applied to the models. The distribution for C_dS/m was truncated at 5.0×10^{-6} and 50.0×10^{-6} m^2 kg^{-1} to set realistic limits for the range of values explored by the Bayesian sampling algorithm. Compressibility (r) was fixed as 0.38 Pa^{-1} that was estimated for northern bottlenose whales *Hyperoodon ampullatus* (Miller et al., 2016).

We evaluated a set of models in order to explore the variability in tissue body density, the drag term and diving lung volume following Miller et al. (2016). See JAGS script in the appendix of Miller et al. (2016) for the detailed structure of the hierarchical model. All models were sampled in three independent chains, with 48,000 iterations each. The first 24,000 samples were discarded for burn-in, and the remaining posterior samples were downsampled by a factor of 36. Convergence was assessed for each parameter by using trace history and Brooks–Gelman–Rubin diagnostic plots (Brooks and Gelman, 1998). Model selection was based on the deviance information criterion (DIC), with lower values indicating a better model fit relative to model complexity.

Effect of buoyancy on optimal swim speed

The theoretical actuator disc model predicts that the optimal speed (minimum COT swim speed) increases with deviations from neutral buoyancy (Miller et al., 2012). To investigate whether buoyancy affects optimal speed, we calculated buoyancy F_B (N) during ascent, with active stroking, according to the following equation, modified from Eqn 2:

$$F_B = \left(\frac{\rho_{sw}}{\rho_{tissue}(d)} - 1\right) \cdot \boldsymbol{g} \cdot m + V_{air} \cdot \boldsymbol{g} \cdot \frac{\rho_{sw} - \rho_{air} \cdot (1 + 0.1d)}{(1 + 0.1d)}. \quad (4)$$

We averaged swim speed, pitch, depth and $F_B \cdot \sin(p)$ (buoyancy along the swimming path of animals) at 10 s intervals during the propulsive swimming of ascent phases. We used the global (i.e. species average across individuals) estimate for volume of air per unit of mass and tissue body densities estimated for each individual in the most parsimonious model (i.e. the lowest DIC model). We assumed the same body mass (1000 kg) for all whales for this calculation. The effect of buoyancy was assessed using linear mixed models. We assigned buoyancy, depth and the interaction of depth and buoyancy as fixed effects and individuals as a random effect. Akaike's information criterion (AIC) was used to select the most parsimonious model.

All statistical analyses were performed using R version 3.2.1 (R Development Core Team 2008; www.r-project.org/). We report mean±s.d. values.

RESULTS

We recorded fine-scale underwater movements of 18 long-finned pilot whales and obtained a total of 160.8 h diving data: 16 individuals were tagged with DTAG, and two individuals were tagged with the speed data-logger PD3GT (Table 1). The tagged whales spent 16±15% of their time in deep dives (n=18 whales) that exceeded a maximum depth of 250 m (Fig. 1). Dive duration and dive depth of deep dives (>250 m) were 536±90 s and 444±85 m, respectively (n=140 dives). The maximum dive duration and depth were 821 s and 617 m, respectively.

Swim speed and stroking patterns

During deep dives (maximum dive depth, >250 m), tagged pilot whales predominantly employed stroking during ascent (20±10% of ascent time was spent gliding, n=140 dives; Table 1), and the mean swim speed during ascent phases was 2.7±0.3 m s^{-1} (pitch, 69±8 deg, n=135 dives). In contrast, they employed prolonged glides or stroke-and-glide throughout descent phases (63±18% of descent time was spent gliding, n=140 dives), and the average speed was 2.9±0.4 m s^{-1} (pitch, −59±8 deg, n=123 dives).

Deep dives occasionally had short events of elevated speed over 10 s intervals that were accompanied by increased stroking rate. In order to identify these events, we defined sprints as any interval of 10 s or more with a mean speed greater than 4.2 m s^{-1}, i.e. 5 s.d. greater than the mean sustained speed of propulsive swimming (i.e. mean speed of ascent phases, 2.7±0.3 m s^{-1}). No sprints were noted in 76% of deep dives (n=106/140 dives), and 19% of dives (n=27/140 dives) included only one sprint (maximum number of sprints, 3 per dive). These events often occurred at the end of descent (n=31/47 sprints). The maximum speed during sprints was 5.8±1.0 m s^{-1} (n=47 sprints, maximum 9.3 m s^{-1}).

Drag coefficient

Drag coefficient C_d was estimated from two whales tagged with the speed data logger PD3GT (0.0037±0.0009, median=0.0035, range=0.0022–0.0070, n=31 glides; Fig. 2). We estimated C_d over the wide range of swim speeds (0.7–3.1 m s^{-1}). The estimated C_d was consistent with, and not lower, than that of other species (Fig. 2).

Estimates of body density: negative tissue body density of tagged animals

A total of 2027 gliding periods from 14 tagged animals were successfully identified at depths ranging from 1 to 553 m, with a wide range of swim speeds (0.5–5.7 m s^{-1}). Most individual tag records had more than 50 glides (range, 26–374; Table 2).

Bayesian model estimates (means of the posterior distributions) were compared across the different models, which differed in how tissue body density, diving air volume and drag coefficient terms were allowed to vary between individuals and dives. The most parsimonious model with the lowest DIC evaluated global plus individual variations in tissue body density and drag terms, as well as global plus dive-by-dive variability in diving lung volume. The model had a DIC value of −6394, and it decreased from a DIC value of 13,232 of the model containing only global values (i.e. fixed values) for all three terms.

The posterior mean of the global drag term (C_dS/m) was 22×10^{-6} m^2 kg^{-1}, overlapping, but slightly (2.0×10^{-6} m^2 kg^{-1}) lower than the mean of the specified normal prior. Most individual posterior means for the drag term were 20×10^{-6} to 25×10^{-6} m^2 kg^{-1} and ranged overall from 15×10^{-6} to 28×10^{-6} m^2 kg^{-1} (Table 2).

The global species mean (±95% CI) tissue density was estimated at 1038.8±1.6 kg m^{-3}. Individual posterior mean values for tissue density ranged from 1034.6 to 1044.4 kg m^{-3}, with ±95% CI widths of 0.3–1.6 kg m^{-3} (Table 2). Estimated tissue densities of all tagged animals were clearly higher than the density of seawater (1027.6±0.6 kg m^{-3}).

The proportion of time spent gliding during ascent (20±10%, n=140 dives; Table 1) was substantially lower than that during descent (63±18%, n=140 dives; Table 1), indicating that tagged whales show negative buoyancy during most of their transit time to deep depths (>250 m). The mean global diving gas volume was estimated at 34.6±0.6 ml kg^{-1}, indicating somewhat larger gas

Journal of Experimental Biology (2017) 220, 3802-3811 doi:10.1242/jeb.158287

Table 1. Summary of dive parameters for deep dives (>250 m) recorded from 18 tagged long-finned pilot whales

Whale ID	Date	Tag type	Deployment duration (h)	*n*	Dive depth (m)	Dive duration (min)	Glide ratio		Swim speed			
							Ascent (%)	Descent (%)	Ascent (m s^{-1})*	*n*	Descent (m s^{-1})*	*n*
gm08_154d	4 Jun 2008	DTAG	8.3	4	430±118	8.2±0.8	8±1	74±13	2.8±0.2	4	2.4±0.5	3
gm08_159a	7 Jun 2008	DTAG	10.4	15	382±38	10.2±1.9	23±5	81±10	2.5±0.2	15	2.9±0.6	14
gm09_137b	17 May 2009	DTAG	8.4	1	287	8.7	26	57	2.2	1	–	0
gm09_137c	17 May 2009	DTAG	8.4	1	297	7.4	11	45	–	0	–	0
gm09_138a	18 May 2009	DTAG	11.0	13	421±17	9.1±0.7	9±2	74±9	2.6±0.2	13	2.8±0.2	13
gm09_138b	26 May 2009	DTAG	17.4	11	404±43	9.0±1.0	19±7	59±12	2.6±0.2	11	2.5±0.3	9
gm09_146a	26 May 2009	DTAG	2.2	9	294±5	8.1±1.0	20±4	63±11	2.9±0.2	9	2.5±0.3	7
gm09_156b	5 Jun 2009	DTAG	17.9	23	473±87	8.4±1.3	26±7	50±15	2.6±0.2	22	3.0±0.5	21
gm10_143a	23 May 2010	DTAG	10.1	5	445±46	8.9±0.8	17±5	57±16	2.5±0.2	5	2.5±0.3	5
gm10_152c	1 Jun 2010	DTAG	1.5	1	414	8.6	44	69	–	0	–	0
gm10_157a	6 Jun 2010	DTAG	4.0	4	535±33	9.4±1.1	14±2	29±18	2.7±0.2	4	3.1±0.2	4
gm10_157b	6 Jun 2010	DTAG	12.0	13	511±78	9.3±1.8	11±2	61±24	3.0±0.3	12	2.8±0.4	11
gm10_158a	7 Jun 2010	DTAG	2.1	6	435±77	9.1±2.0	25±8	48±12	2.8±0.3	5	3.2±0.6	5
gm13_137a	17 May 2013	DTAG	8.6	0	–	–	–	–	–	0	–	0
gm13_149a	29 May 2013	DTAG	5.1	8	446±61	10.1±1.6	13±2	81±6	2.7±0.4	8	3.2±0.3	7
gm13_169a	18 Jun 2013	DTAG	7.9	0	–	–	–	–	–	0	–	0
LpW_10pm1N	24 May 2010	PD3GT	5.7	4	549±24	9.2±1.1	23±1	71±18	3.2±0.3	4	3.4±0.3	4
LpW_10pm2N	6 Jun 2010	PD3GT	19.8	22	493±58	8.3±1.4	33±10	67±18	2.8±0.3	22	3.1±0.4	20

n is the number of dives.
*Mean swim speed was calculated when the mean pitch was 45 deg.

volume than that of sperm whales *Physeter macrocephalus* (26.4 ml kg^{-1}; Miller et al., 2004a) and northern bottlenose whales (27.4 ml kg^{-1}; Miller et al., 2016). Individual means of the dive-by-dive estimates ranged between 27.4 and 38.9 ml kg^{-1}.

Effect of negative buoyancy on transit speed during active swimming

To investigate whether deviations from neutral buoyancy increase swim speed, we determined the relationship between total body buoyancy and swim speed during active swimming of ascent phases (Fig. 3). The most parsimonious model (lowest AIC model) included only buoyancy (Table 3). The swim speed of tagged pilot whales gradually decreased as they approached the water surface during ascent because the buoyancy of the whales became close to neutral buoyancy owing to the expansion of gases carried by the animal. Assuming that pilot whales swam at optimal speed during ascent, this result indicates that buoyancy affected their optimal swim speed. The intercept of this correlation was 2.3±0.15 m s^{-1}

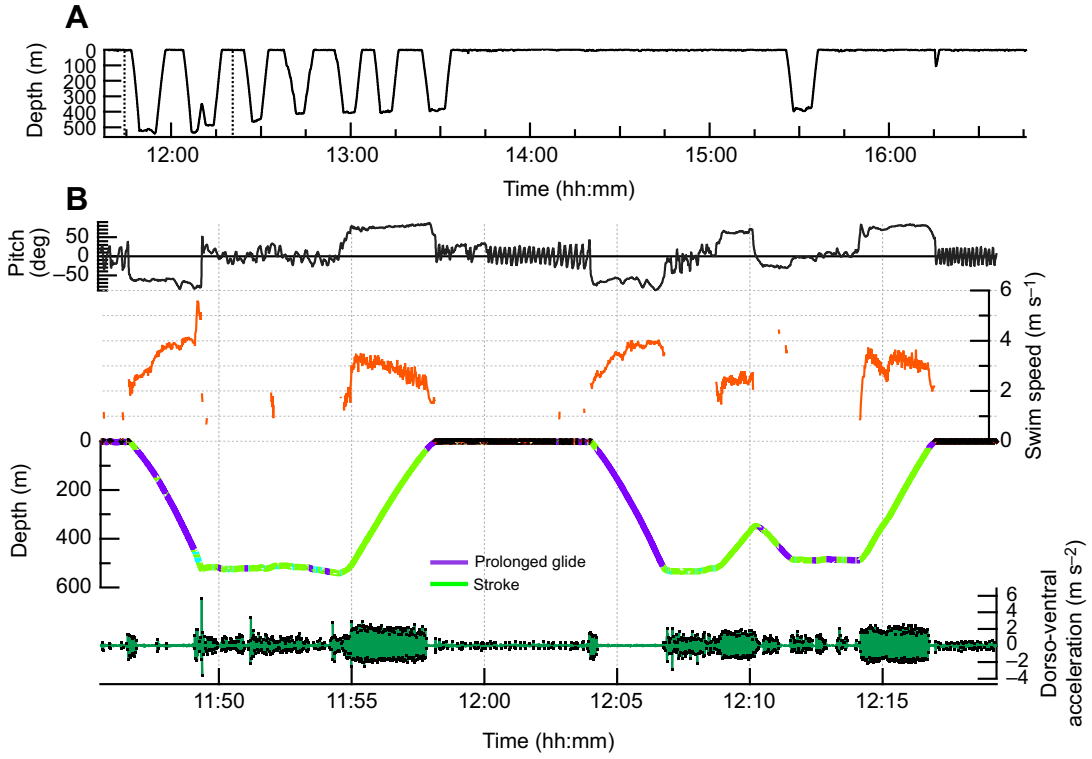

Fig. 1. Typical examples of dive profiles of a tagged long-finned pilot whale (whale ID, gm13_149a). (A) Entire record of dive depth. (B) Enlarged profile of the graph between the dashed lines in A. The tagged whale employed prolonged gliding during descent and continuous stroking during ascent.

Journal of Experimental Biology (2017) 220, 3802-3811 doi:10.1242/jeb.158287

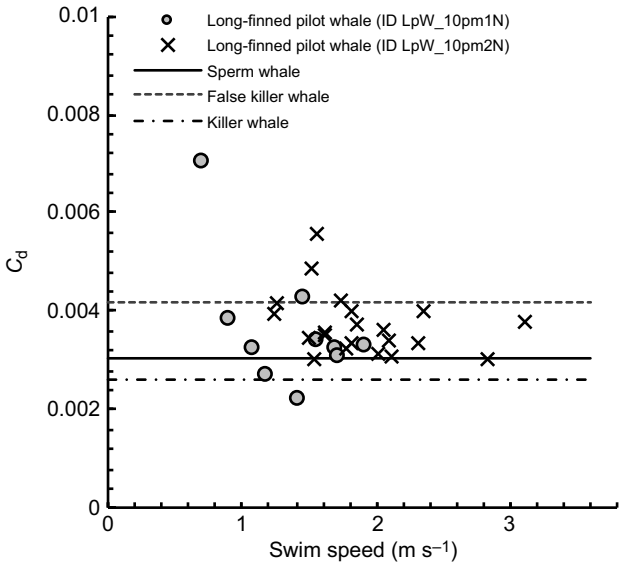

Fig. 2. Drag coefficient (C_d) of two tagged long-finned pilot whales estimated from deceleration during horizontal glides. The median value was 0.0035, similar to that reported for other species (0.0042, false killer whales: Fish, 1998; 0.0026, killer whales: Fish, 1998; 0.0031, sperm whales: Miller et al., 2004a).

(±95% confidence interval), which would indicate the optimal swim speed of pilot whales at neutral buoyancy.

DISCUSSION

Diving mammals are expected to descend and/or ascend at optimal speed to minimize the cost of transport, which could enable them to maximize the time spent at foraging depths. The rate of oxygen consumption is predicted to increase as a cubic function of swim speed during stroking (e.g. Kooyman, 1989; Otani et al., 2001). Therefore, how animals choose their swim speed is important to understand their foraging strategy via its effect on their energy budget. Another key aspect of energetic expenditure is load against buoyancy that can affect the stroking patterns of swimmers, with increased gliding when buoyancy aids movement (Skrovan et al., 1999; Williams et al., 2000; Miller et al., 2004a). Although gliding can reduce the COT relative to active swimming (Williams et al., 2000), the key consideration for round-trip COT in divers is that any buoyancy force that aids movement in one direction of the transit to/from depth will hinder movement in the opposing direction (Miller et al., 2012). A recent study indicates that neutral buoyancy minimizes the COT (Sato et al., 2013). We analysed the detailed swimming behaviours of tagged long-finned pilot whales and found that they show (1) high transit speed during propulsive swimming, (2) similar drag coefficient to that of other whales, (3) strong negative buoyancy, and (4) a correlation between transit speed and buoyancy. We compared the transit speed of tagged animals with that of other cetaceans and considered the diving metabolic rate of long-finned pilot whales. The implications for the diving and foraging strategies of long-finned pilot whales were also considered.

High diving metabolic rate indicated by high-speed transit to depth

The transit speed from surface to depth in tagged species ranging from 0.5 kg seabirds to 30,000 kg sperm whales has been estimated to be 1–2 m s^{-1} during propulsive swimming (Sato et al., 2007). Speed was suggested to be independent of body size (Sato et al., 2007), but recent tagging studies on a range of marine vertebrates have found propulsive speed (minimum COT swim speed) at transit to be proportional to body mass (Sato et al., 2010; Watanabe et al., 2011). Assuming the body mass of tagged long-finned pilot whales to be within the range 300–2000 kg, the optimal swim speed was predicted to be 1.4–1.7 m s^{-1} (Fig. 4) based on the equation for marine mammals (speed=0.78mass$^{0.10}$; Watanabe et al., 2011). In contrast, the observed transit speed during propulsive swimming in the ascent phases was 2.7±0.29 m s^{-1}, which was clearly higher

Table 2. Bayesian estimates from the best model (No.12) for 14 tagged long-finned pilot whales

Whale ID	Body length (cm)*	Body mass (kg)*	VO of body size‡	No. of glides <100 m	No. of glides ≥100 m	Body density (kg m^{-3})	C_dS/m (10^{-6} m^2 kg^{-1})	Volume of air (ml kg^{-1})
gm08_154d	–	–	–	51	16	1039.8±1.3	28±3.0	27.4±18.1
gm08_159a	–	–	Large	105	85	1041.9±1.1	19±1.3	37.9±16.4
gm09_137b	440	925	Medium	76	4	–	–	–
gm09_137c	–	–	Small	70	0	–	–	–
gm09_138a	–	–	Medium	74	66	1038.9±1.4	15±1.9	31.1±19.5
gm09_138b	400	740	Small	105	110	1037.1±0.7	26±1.2	35.9±20.3
gm09_146a	–	–	–	25	25	1039.7±1.5	25±2.1	38.9±21.0
gm09_156b	–	–	Large	144	85	1037.1±0.6	21±1.0	36.7±22.0
gm10_143a	490	1236	Medium	82	40	1035.9±1.0	24±1.9	34.7±20.0
gm10_152c	–	–	–	23	3	–	–	–
gm10_157a	–	–	–	33	9	1038.1±1.6	24±2.5	33.3±19.2
gm10_157b	530	1477	Medium	99	80	1038.3±0.9	22±1.5	37.9±26.6
gm10_158a	510	1340	–	19	24	1034.6±1.6	25±2.9	35.2±22.7
gm13_137a	380	651	Small	43	2	–	–	–
gm13_149a	–	–	Large	43	42	1040.4±1.6	15±1.8	29.4±15.9
gm13_169a	–	–	Large	102	13	1037.3±1.1	23±3.0	32.9±19.1
LpW_10pm1N	490	1230	–	139	37	1044.4±0.7	19±0.8	35.6±20.6
LpW_10pm2N	530	1475	–	248	126	1040.6±0.3	21±0.4	34.8±19.5

Body density, the drag term C_dS/m (where C_d is the coefficient of drag, S is surface area and m is body mass) and volume of air are given as means±95% credible interval (CI).

Whales having only a few deep glides (<5) were excluded.

*Body length (L) was estimated from photogrammetry and the length was subsequently converted to an estimate of whale's mass (m) using Lockyer's equation (m=0.00023$L^{2.501}$) (see 'Estimation of body mass and surface area' in Materials and methods for details).

‡The size of tagged animals was visually categorized (VO, visual observation).

Journal of Experimental Biology (2017) 220, 3802-3811 doi:10.1242/jeb.158287

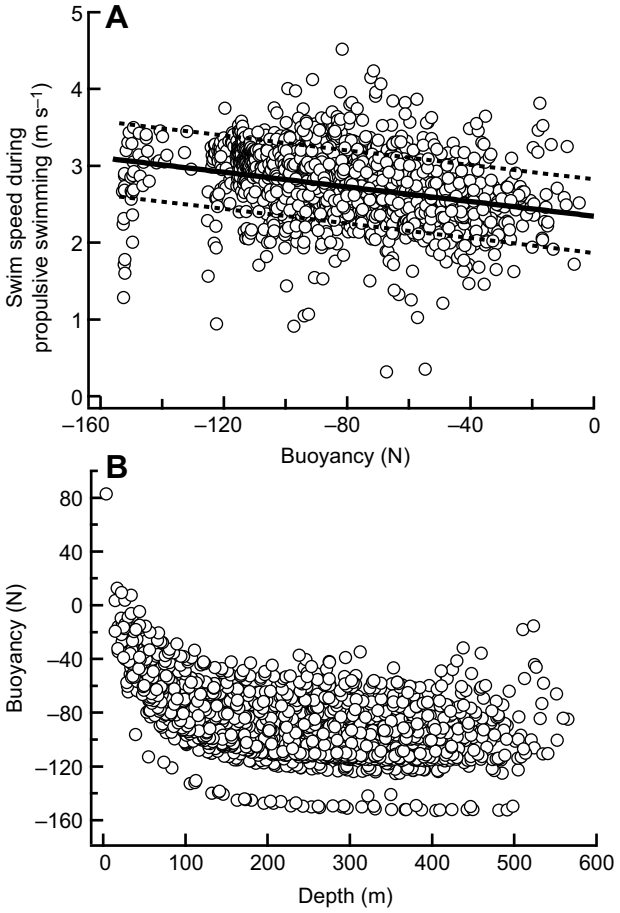

Fig. 3. Effect of negative buoyancy on transit speed. (A) Transit speed during propulsive swimming plotted against buoyancy along the swimming path of animals [F_B·sin(p)] at the ascent of deep dives. (B) Buoyancy along the swimming path of animals [F_B·sin(p)] plotted against depth during ascent transit. Linear regression line of swim speed on buoyancy: speed=−0.00477±0.00081×buoyancy+2.3±0.15 (±95% confidence interval). Dashed lines show 95% confidence interval of the linear regression line. See Table 3 for statistical models.

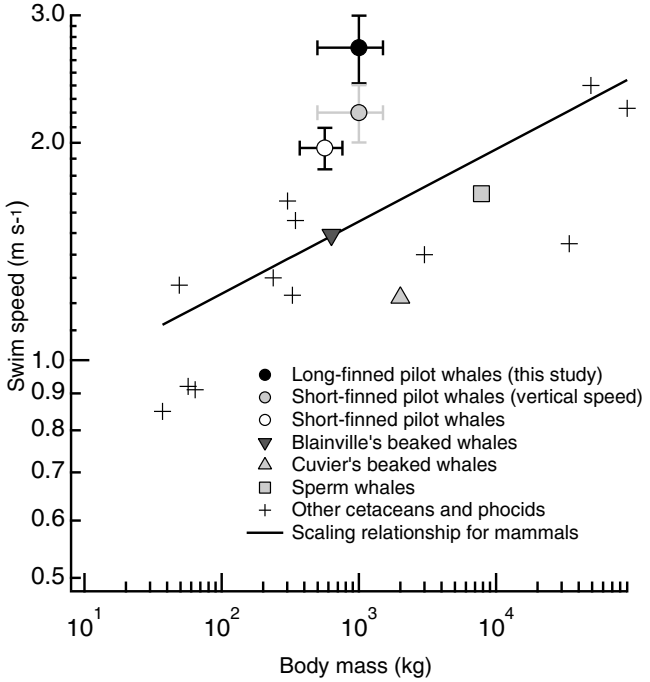

Fig. 4. Comparison of transit speed among deep-diving toothed whales. Swim speed during the propulsive swimming phase (descent or ascent) plotted against body mass (modified from Watanabe et al., 2011). The grey square shows the swim speed of sperm whales, measured using propeller rotation of the speed data-loggers (Watanabe et al., 2011). Swim speed of beaked whales was calculated as the mean pitch and depth change rate at ascent of deep foraging dives (Tyack et al., 2006). The white circle shows swim speed of short-finned pilot whales, measured using propeller rotation of the speed data-loggers, W2000-PD3GT, during the ascent of deep dives (>250 m; K.A., unpublished data). The grey circle shows the vertical swim speed of short-finned pilot whales during ascent (Aguilar Soto et al., 2008).

than the optimal swim speed predicted from body mass (Fig. 4). The external work biomechanical model predicts that the optimal speed during active swimming is proportional to (basal metabolic rate/drag)$^{1/3}$ (Sato et al., 2010; Watanabe et al., 2011). Assuming that tagged pilot whales swam at optimal speed, the high transit speed therefore suggests either (1) a high diving metabolic rate and/or (2) a low drag coefficient compared with that in other marine mammals. The drag coefficient estimated in this study had a median value of 0.0035, which was not clearly lower than those of other cetaceans (0.0042, false killer whale, *Pseudorca crassidens*: Fish, 1998; 0.0026, killer whale, *Orcinus orca*: Fish, 1998; 0.0031, sperm whale: Miller et al., 2004a; Fig. 2). According to the theoretical models, higher transit speed and a consistent drag coefficient specifically indicate that the basal metabolic rate of diving long-finned pilot whales could be elevated compared with those in other species. Therefore, the greater speed employed during locomotion leads to the prediction that the diving metabolic rate is higher than that in other marine mammals during active swimming, owing to the greater basal and locomotor costs. The dive duration of the tagged whales (mean, 8.9 min) was shorter than that in other marine mammals of similar or smaller size (e.g. female southern elephant seals, *Mirounga leonina*, mean dive duration, 20 min; mean body mass, 342 kg; Hindell et al., 2000); this also supports the finding that pilot whales maintained higher diving metabolic rate than that in other deep-diving mammals.

Table 3. Fit of linear mixed models to data on propulsive swimming at ascent phases of tagged pilot whales indicated by Akaike's information criterion (AIC)

Model	AIC
Swim speed~null	1675
Swim speed~depth	1641
Swim speed~buoyancy	1561
Swim speed~depth+buoyancy	1580
Swim speed~depth×buoyancy	1605

Does buoyancy affect optimal swim speed?

There are two biomechanical models that have been used to explain optimal swim speed: the external work model and the actuator disc model. (1) The external work model predicts that optimal speed during active swimming is proportional to (basal metabolic rate/drag)$^{1/3}$, but not buoyancy, as mentioned above (Sato et al., 2010; Watanabe et al., 2011). (2) The actuator disc model predicts that optimal speed is proportional to basal metabolic rate and increases with deviations from neutral buoyancy (Miller et al., 2012). Our results showed that the swim speed of tagged whales gradually decreases as they move closer to the sea surface during ascent because the buoyancy of the whales becomes closer to neutral

Journal of Experimental Biology (2017) 220, 3802-3811 doi:10.1242/jeb.158287

buoyancy owing to the expansion of gases (Fig. 3). This result indicates that buoyancy does affect the optimal swim speed and supports the actuator disc model. Negative buoyancy of tagged pilot whales could therefore be an additional contributing factor for the high speed noted during active swimming. However, our results showed that the predicted transit speed of whales with neutral buoyancy (intercept of regression, 2.3±0.15 m s^{-1}, ±95% confidence interval) was still substantially higher than the optimal speed expected from the body mass of other mammals (1.4–1.7 m s^{-1}).

Comparison of transit speed and dive duration among deep-diving toothed whales

A few dozen species of deep-diving toothed whales utilize prey resources in mesopelagic water. Although little is known about the swimming kinematics of deep-diving toothed whales, the diving behaviour of several species such as sperm whales, beaked whales, pilot whales and northern bottlenose whales has been investigated in detail by using animal-borne recorders (e.g. Amano and Yoshioka, 2003; Miller et al., 2004b; Tyack et al., 2006; Watwood et al., 2006; Aoki et al., 2007, 2012, 2015; Aguilar Soto et al., 2008). Sperm whales routinely dive to depths of 400–1300 m for half an hour or longer (Amano and Yoshioka, 2003; Miller et al., 2004b; Watwood et al., 2006; Aoki et al., 2007). Northern bottlenose whales dive approximately every 80 min to over 800 m (maximum, 1453 m) and up to 70 min in duration (Hooker and Baird, 1999). Beaked whales (including *Ziphius cavirostris* and *Mesoplodon densirostris*) are known to be extreme divers. They perform the deepest and longest average foraging dives among any marine mammals (835–1070 m, 47–58 min; Tyack et al., 2006). Short-finned pilot whales, *Globicephala macrorhynchus*, routinely perform foraging dives with a median duration and depth of 15 min and 762 m, respectively (Aguilar Soto et al., 2008). To discuss the diving strategy of long-finned pilot whales, we compared the relationship between (1) dive duration and body mass and (2) transit speed during propulsive swimming and body mass among deep-diving toothed whales.

Because of the substantial differences in body size of deep-diving toothed whales mentioned above, we expected differences in the aerobic dive limit (ADL), which is the dive duration that can be performed aerobically (Kooyman et al., 1980; Williams et al., 2000), among these species. Although the ADL has not been experimentally measured in these species, an estimated ADL can be calculated by scaling up measurements obtained from other cetaceans for which the ADL has been measured (see Watwood et al., 2006; Tyack et al., 2006). The lean mass (m)-specific basal metabolic rate of mammals scales as $m^{-0.25}$ (Kleiber, 1975), whereas oxygen stores scale in a linear fashion. Therefore, larger animals can dive longer aerobically than smaller animals (Castellini et al., 1992). To compare the dive duration among deep-diving toothed whales, we estimated the relationship between calculated ADL (cADL) and body mass by using data for Weddell seals (23 min, 387.4 kg; Williams et al., 2004), known deep divers; narwhals (22 min, 923 kg; Williams et al., 2011); and beluga whales (10 min, 776 kg; Shaffer et al., 1997). Assuming that diving metabolic rate scales with lean body mass in a manner similar to the basal metabolic rate, and that animals contain similar mass-specific oxygen stores to those of the measured animals, the ADL of the whale can be estimated as follows:

$$\mathrm{ADL}_{\mathrm{animals}} = \mathrm{ADL}_{\mathrm{measured\ animals}}\left(m_{\mathrm{measured\ animals}}/m_{\mathrm{animals}}\right)^{-0.25}. \quad (5)$$

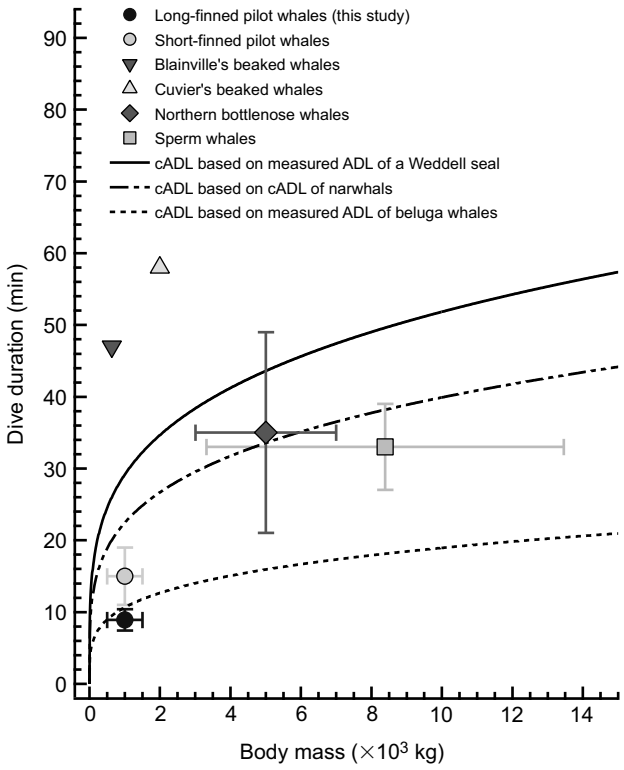

Fig. 5. Comparison of dive duration and calculated aerobic dive limit (cADL) among deep-diving toothed whales. The mean dive duration of foraging dives (695±247 m) was 33±6 min for tagged female or immature sperm whales (Aoki et al., 2012). Estimated body length of these tagged animals (6–10 m) was converted to an estimate of animal mass in metric tons (10^3 kg) using Lockyer's equation for sperm whales (1.25×0.0196×length$^{2.74}$; length in m; Lockyer, 1976), where the 1.25 multiplier accounts for blood loss (Rice, 1989; Miller et al., 2004a). Deep foraging dives (median: 762 m, range: 538–1019 m) of short-finned pilot whales had a median duration of 15 min (11–21 min; Aguilar Soto et al., 2008). The mean dive depth and dive duration of deep dives (>500 m) in tagged northern bottlenose whales was 960±447 m and 35±14 min, respectively (n=57 dives from 12 individuals; T.N., unpublished data; for details of data collection, see Miller et al., 2016). Average dive duration of foraging dives is 47 min for Blainville's beaked whale and 58 min for Cuvier's beaked whale (Tyack et al., 2006).

Marine mammals have been hypothesized to perform the majority of their dives aerobically (Kooyman et al., 1980), but both beaked whales dived beyond their calculated ADL based on the extrapolation from all three species (Fig. 5). The mean dive duration of northern bottlenose whales was slightly over their ADL estimated from narwhals. The average dive duration of sperm whales was within their ADL estimated from the Weddell seals and narwhals, but not from beluga whales. The median dive duration (15 min) of short-finned pilot whales was about two-thirds of their calculated ADL based on the data for narwhals. They performed sprints reaching 4–9 m s^{-1}, possibly to chase prey, at the deepest portion of the dive, which might be responsible for their relatively short duration of dives (Aguilar Soto et al., 2008). Indeed, short-finned pilot whales have muscle morphology supporting high activity events (Velten et al., 2013). Tagged long-finned pilot whales in this study rarely sprinted, but their average diving duration was less than that of short-finned pilot whales and was close to the cADL based on extrapolation from beluga whales, but shorter than the ADL extrapolated from Weddell seals and narwhals (Fig. 5). This indicates that long-finned pilot whales have similar diving metabolic rate and/or diving capacity to that of beluga whales rather than other deep-diving toothed whales.

We assessed the cruising speed during propulsive swimming for the transit between surface and depth against the body mass of deep-diving toothed whales (Fig. 4). The cruising speed of sperm whales, beaked whales and bottlenose whales was similar to the optimal swim speed expected from their body mass, indicating that their diving metabolic rate was similar to that expected from their body mass. Although sperm whales occasionally accelerated up to approximately 7.0 m s^{-1}, with rapid changes in body posture and sharp turns possibly to catch prey (Amano and Yoshioka, 2003; Aoki et al., 2012), they transited between the surface and depth at consistently lower speeds. Both beaked whales maintained a relatively steady and slow vertical speed (1.5 m s^{-1}; Tyack et al., 2006). These species seem to be particularly adapted to conserve energy during transit phases to maximize foraging duration. Deep-diving animals should benefit by transiting to and from depth at the optimal swim speed, because this strategy maximizes the amount of oxygen available for efficient aerobic metabolism at depth (Thompson et al., 1993). The large diving capacity of sperm whales compared with that of beaked whales might allow them to occasionally sprint to catch prey and dive within the ADL. In contrast, the observed cruising speeds of both short-finned pilot whales (Aguilar Soto et al., 2008) and long-finned pilot whales (this study) were higher than those expected from their body mass, indicating higher diving metabolic rate of both species than that expected by their body mass alone. In addition, the transit speeds of long-finned pilot whales in this study were higher than those previously reported for short-finned pilot whales (Aguilar Soto et al., 2008). We simulated the basal metabolic rate of diving long-finned pilot whales under a wide range of optimal swim speeds by using empirical allometric relationships between swim speed and basal metabolic rate from Watanabe et al. (2011). The predicted transit speed of tagged whales with neutral buoyancy (2.3 m s^{-1}) was used to estimate the basal metabolic rate from the empirical allometric relationships of other marine mammals [speed=0.60(basal metabolic rate)$^{0.14}$; Watanabe et al., 2011]. Assuming that the body mass of tagged animals was 1000 kg, the estimated basal metabolic rate was roughly 10 times higher than that expected from body mass (basal metabolic rate=6.78×$m^{0.75}$; Watanabe et al., 2011).

Our results indicate that long-finned pilot whales maintain high diving metabolic rate during deep foraging dives. They might have a 'spend more, gain more' strategy. This differs from that in other deep-diving toothed whales, which might reduce the costs of locomotion, allowing resources to be redirected towards hunting in mesopelagic waters. The mitochondrial density of epaxial (swimming) muscles of pilot whales has been shown to be higher than that in other mesopelagic foragers (Spitz et al., 2012), which supports our results. However, more information is needed to understand the prey acquisition of pilot whales to completely elucidate their energy balance. We predict that the higher activity levels of pilot whales during dives should enable them to obtain more energy from prey than other low-cost strategy mesopelagic foragers.

Acknowledgements

We thank L. Kleivane, A. Bocconcelli, R. Antunes, A. C. Alves, M. Bivins, C. Cure, S. Kuningas, M. Oudejans, P. White, and all science and crew members of MS Strønstad and R/V HU Sverdrup II who helped with the fieldwork. R. Beaton, M. Simon and A. Wallis helped with the tag design. Our laboratory members provided many helpful suggestions.

Competing interests

The authors declare no competing or financial interests.

Author contributions

Methodology: K.A., T.N., S.I., P.J.O.M.; Validation: T.N., S.I.; Formal analysis: K.A.; Investigation: K.A., K.S., T.N., P.J.O.M.; Data curation: K.A., S.I.; Writing - original draft: K.A., P.J.O.M.; Writing - review & editing: K.A., K.S., S.I., P.J.O.M.; Project administration: P.J.O.M.; Funding acquisition: K.S., P.J.O.M.

Funding

The US Office of Naval Research and Strategic Environmental Research and Development Program (SERDP) supported the fieldwork as a part of the 3S study collaboration. This study was also supported by the program Bio-Logging Science of the University of Tokyo (UTBLS).

References

Aguilar Soto, N., Johnson, M. P., Madsen, P. T., Díaz, F., Domínguez, I., Brito, A. and Tyack, P. (2008). Cheetahs of the deep sea: deep foraging sprints in short finned pilot whales off Tenerife (Canary Islands). *J. Anim. Ecol.* **77**, 936-947.

Amano, M. and Yoshioka, M. (2003). Sperm whale diving behavior monitored using a suction-cup-attached TDR tag. *Mar. Ecol. Prog. Ser.* **258**, 291-295.

Aoki, K., Amano, M., Yoshioka, M., Mori, K., Tokuda, D. and Miyazaki, N. (2007). Diel diving behavior of sperm whales off Japan. *Marine Mar. Ecol. Prog. Ser.* **349**, 277-287.

Aoki, K., Watanabe, Y. Y., Crocker, D. E., Robinson, P. W., Biuw, M., Costa, D. P., Miyazaki, N., Fedak, M. A. and Miller, P. J. O. (2011). Northern elephant seals adjust gliding and stroking patterns with changes in buoyancy: validation of at-sea metrics of body density. *J. Exp. Biol.* **214**, 2973-2987.

Aoki, K., Amano, M., Mori, K., Kourogi, A., Kubodera, T. and Miyazaki, N. (2012). Active hunting by deep-diving sperm whales: 3D dive profiles and maneuvers during bursts of speed. *Mar. Ecol. Prog. Ser.* **444**, 289-301.

Aoki, K., Amano, M., Kubodera, T., Mori, K., Okamoto, R. and Sato, K. (2015). Visual and behavioral evidence indicates active hunting by sperm whales. *Mar. Ecol. Prog. Ser.* **523**, 233-241.

Baird, R. W., Borsani, J. F., Hanson, M. B. and Tyack, P. L. (2002). Diving and night-time behavior of long-finned pilot whales in the Ligurian Sea. *Mar. Ecol. Prog. Ser.* **237**, 301-305.

Beck, C. A., Bowen, W. D. and Iverson, S. J. (2000). Seasonal changes in buoyancy and diving behaviour of adult grey seals. *J. Exp. Biol.* **203**, 2323-2330.

Biuw, M., McConnell, B., Bradshaw, C. J. A., Burton, H. and Fedak, M. A. (2003). Blubber and buoyancy: monitoring the body condition of free-ranging seals using simple dive characteristics. *J. Exp. Biol.* **206**, 3405-3423.

Bloch, D., Zachariassen, M. and Zachariassen, P. (1993). Some external characters of the long-finned pilot whale off the Faroe Islands and a comparison with the short-finned pilot whales. *Rep. Int. Whal. Comm. Sp Issue* **14**, 117-135.

Bose, N., Lien, J. and Ahia, J. (1990). Measurements of the bodies and flukes of several cetacean species. *Proc. R. Soc. B Biol. Sci.* **242**, 163-173.

Brooks, S. P. and Gelman, A. (1998). General methods for monitoring convergence of iterative simulations. *J. Comput. Graphical Stat.* **7**, 434-455.

Buckland, S. T., Bloch, D., Cattanach, K. L., Gunnlaugsson, T., Hoydal, K., Lens, S. and Sigurjónsson, J. (1993). Distribution and abundance of long-finned pilot whales in the North Atlantic, estimated from NASS-1987 and NASS-89 data. *Rep. Int. Whal. Comm. Sp .Issue* **14**, 33-49.

Castellini, M. A., Kooyman, G. L. and Ponganis, P. J. (1992). Metabolic rates of freely diving Weddell seals: correlations with oxy- gen stores, swim velocity and diving duration. *J. Exp. Biol.* **165**, 181-194.

Curren, K. C. (1992). Designs for swimming: morphometrics and swimming dynamics of several cetacean species. *Masters thesis*, Memorial University of Newfoundland, St John's, Canada.

Desportes, G. and Mouritsen, R. (1993). Preliminary results on the diet of long-finned pilot whales off the Faroe Islands. *Rep. Int. Whal. Comm. Sp. Issue* **14**, 305-324.

Ellington, C. P. (1984). The aerodynamics of hovering insect flight. V. A vortex theory. *Philos. Trans. R. Soc. B Biol. Sci.* **305**, 115-144.

Feldkamp, S. D. (1987). Swimming in the California sea lion: morphometrics, drag and energetics. *J. Exp. Biol.* **131**, 117-135.

Fish, F. E. (1998). Comparative kinematics and hydrodynamics of odontocete cetaceans: morphological and ecological correlates with swimming performance. *J. Exp. Biol.* **201**, 2867-2877.

Fish, F. E. and Rohr, J. J. (1999). *Review of dolphin hydrodynamics and swimming performance*. Space and Naval Warfare Systems Command Technical Report 1081, San Diego.

Gallon, S. L., Sparling, C. E., Georges, J. Y., Fedak, M. A., Biuw, M. and Thompson, D. (2007). How fast does a seal swim? Variations in swimming behaviour under differing foraging conditions. *J. Exp. Biol.* **210**, 3285-3294.

Heide-Jorgensen, M. P., Bloch, D., Stefansson, E., Mikkelsen, B., Ofstad, L. H. and Dietz, R. (2002). Diving behaviour of long-finned pilot whales *Globicephala melas* around the Faroe Islands. *Wild. Biol.* **8**, 307-313.

Hind, A. T. and Gurney, W. S. C. (1997). The metabolic cost of swimming in marine homeotherms. *J. Exp. Biol.* **200**, 531-542.

Hindell, M. A., Lea, M. A., Morrice, M. G. and MacMahnon, C. R. (2000). Metabolic limits on dive duration and swimming speed in the southern elephant seal *Mirounga leonina*. *Physio. Biochem. Zool.* **73**, 790-798.
Hooker, S. K. and Baird, R. W. (1999). Deep-diving behaviour of the northern bottlenose whale, *Hyperoodon ampullatus* (Cetacea: *Ziphiidae). Proc. R. Soc. B Biol. Sci.* **266**, 671-676.
Johnson, M. P. and Tyack, P. L. (2003). A digital acoustic recording tag for measuring the response of wild marine mammals to sound. *IEEE J. Ocean. Eng.* **28**, 3-12.
Kleiber, M. (1975). *The Fire of Life: An Introduction to Animal Energetics*. 2nd edn. New York: Robert E. Krieger Publishing Co.
Kleivane, L. (1998). *A New Pneumatic Launching Device ARTS (Aerial Rocket Transmitter System) Especially Developed and Designed to Improve Tagging and Instrumentation of Baleen Whales*. Bodø, Norway: Restech A/S.
Kooyman, G. L. (1989). *Diverse Divers: Physiology and Behavior*. Berlin Heidelberg: Springer-Verlag.
Kooyman, G. L., Wahrenbrock, E. A., Castellini, M. A., Davis, R. W. and Sinnett, E. E. (1980). Aerobic and anaerobic metabolism during voluntary diving in Weddell seals: evidence of preferred pathways from blood chemistry and behavior. *J. Com. Physiol. B.* **138**, 335-346.
Lockyer, C. (1976). Body weights of some species of large whales. *J. Cons. Int. Explor. Mer.* **36**, 259-273.
Lockyer, C. (1993). Seasonal changes in body fat condition of northeast Atlantic pilot whales, and their biological significance. *Rep. Int. Whal. Comm. Sp Issue.* **14**, 325-362.
Miller, P. J. O., Johnson, M. P., Tyack, P. L. and Terray, E. A. (2004a). Swimming gaits, passive drag, and buoyancy of diving sperm whales (*Physeter macrocephalus*). *J. Exp. Biol.* **207**, 1953-1967.
Miller, P. J. O., Johnson, M. P. and Tyack, P. L. (2004b). Sperm whale behaviour indicates the use of echolocation click buzzes 'creaks' in prey capture. *Proc. R. Soc. B Biol. Sci.* **271**, 2239-2247.
Miller, P. J. O., Biuw, M., Watanabe, Y. Y., Thompson, D. and Fedak, M. A. (2012). Sink fast and swim harder! Round trip cost-of-transport for buoyant divers. *J. Exp. Biol.* **215**, 3622-3630.
Miller, P. J. O., Narazaki, T., Isojunno, S., Aoki, K., Smout, S. and Sato, K. (2016). Body density and diving gas volume of the northern bottlenose whale (*Hyperoodon ampullatus*). *J. Exp. Biol.* **219**, 2458-2468.
Otani, S., Naito, Y., Kato, A. and Kawamura, A. (2001). Oxygen consumption and swim speed of the harbor porpoise *Phocoena phocoena*. *Fish. Sci.* **67**, 894-898.
Panneton, M. W. (2013). The mammalian diving response: an enigmatic reflex to preserve life? *Physiol.* **28**, 284-297.
Rice, D. W. (1989). Sperm whale *Physeter macrocephalus* Linnaeus, 1758. In *Handbook of Marine Animals* (ed. S. H. Ridgway and R. Harrison), pp. 177-233. London: Academic Press.
Sato, K., Mitani, Y., Cameron, M. F., Siniff, D. B. and Naito, Y. (2003). Factors affecting stroking patterns and body angle in diving Weddell seals under natural conditions. *J. Exp. Biol.* **206**, 1461-1470.
Sato, K., Watanuki, Y., Takahashi, A., Miller, P. J. O., Tanaka, H., Kawabe, R., Ponganis, P. J., Handrich, Y., Akamatsu, T., Watanabe, Y. et al. (2007). Stroke frequency, but not swimming speed, is related to body size in free-ranging seabirds, pinnipeds and cetaceans. *Proc. R. Soc. B Biol. Sci.* **274**, 471-477.
Sato, K., Shiomi, K., Watanabe, Y., Watanuki, Y., Takahashi, A. Ponganis, P. J. (2010). Scaling of swim speed and stroke frequency in geometrically similar penguins: they swim optimally to minimize cost of transport. *Proc. R. Soc. B Biol. Sci.* **277**, 707-714.
Sato, K., Aoki, K., Watanabe, Y. Y. and Miller, P. J. O. (2013). Neutral buoyancy is optimal to minimize the cost of transport in horizontally swimming seals. *Sci. Rep.* **3**, 2205.
Schmidt-Nielsen, K. (1972). Locomotion: energy cost of swimming, flying, and running. *Science* **177**, 222-228.
Skrovan, R. C., Williams, T. M., Berry, P. S., Moore, P. W. and Davis, R. W. (1999). The diving physiology of bottlenose dolphins (*Tursiops truncatus*) II. Biomechanics and changes in buoyancy at depth. *J. Exp. Biol.* **202**, 2479-2761.
Shaffer, S. A., Costa, D. P., Williams, T. M. and Ridgway, S. H. (1997). Diving and swimming performance of white whales, *Delphinapterus leucas*: an assessment of plasma lactate and blood gas levels and respiratory rates. *J. Exp. Biol.* **200**, 3091-3099.
Suzuki, I., Sato, K., Fahlman, A., Naito, Y., Miyazaki, N. and Trites, A. W. (2014). Drag, but not buoyancy, affects swim speed in captive Steller sea lions. *Biology Open* **3**, 379-386.
Spitz, J., Trites, A. W., Becquet, V., Brind'Amour, A., Cherel, Y., Galois, R. and Ridoux, V. (2012). Cost of living dictates what whales, dolphins and porpoises eat: the importance of prey quality on predator foraging strategies. *PLoS ONE* **7**, e50096.
Thompson, D., Hiby, A. R. and Fedak, M. A. (1993). How fast should I swim? Behavioural implications of diving physiology. *Symp. Zool. Soc. Lond.* **66**, 349-368.
Tyack, P. L., Johnson, M., Aguilar Soto, N., Sturlese, A. and Madsen, P. T. (2006). Extreme diving of beaked whales. *J. Exp. Biol.* **209**, 4238-4253.
UNESCO (1981). *Tenth Report of the Joint Panel on Oceanographic Tables and Standards*. UNESCO Technical Papers in Marine Science, Vol. 36. Paris: UNESCO.
Velten, B. P., Dillaman, R. M., Kinsey, S. T., McLellan, W. A. and Pabst, D. A. (2013). Novel locomotor muscle design in extreme deep-diving whales. *J. Exp. Biol.* **216**, 1862-1871.
Videler, J. J. and Nolet, B. A. (1990). Costs of swimming measured at optimum speed: scale effects, differences between swimming styles, taxonomic groups and submerged and surface swimming. *Comp. Biochem. Physiol. A.* **97**, 91-99.
Vogel, S. (1994). *Life in Moving Fluids: The Physical Biology of Flow*, 2nd edn. Princeton, NJ: Princeton University Press.
Wakeling, J. M. and Ellington, C. P. (1997). Dragonfly flight. III. Lift and power requirements. *J. Exp. Biol.* **200**, 583-600.
Watanabe, Y., Baranov, E. A., Sato, K., Naito, Y. and Miyazaki, N. (2006). Body density affects stroke patterns in Baikal seals. *J. Exp. Biol.* **209**, 3269-3280.
Watanabe, Y. Y., Sato, K., Watanuki, Y., Takahashi, A., Mitani, Y., Amano, M., Aoki, K., Narazaki, T., Takashi, I., Minamikawa, S. et al. (2011). Scaling of swim speed in breath-hold divers. *J. Anim. Ecol.* **80**, 57-68.
Watwood, S. L., Miller, P. J. O., Johnson, M., Madsen, P. T. and Tyack, P. L. (2006). Deep-diving foraging behavior of sperm whales (*Physeter macrocephalus*). *J. Anim. Ecol.* **75**, 814-825.
Weis-Fogh, T. (1972). Energetics of hovering flight in hummingbirds and in *Drosophila*. *J. Exp. Biol.* **56**, 79-104.
Williams, T. M. (1999). The evolution of cost efficient swimming in marine mammals: limits to energetic optimization. *Philos. Trans. R. Soc. B Biol. Sci.* **354**, 193-201.
Williams, T. M., Davis, R. W., Fuiman, L. A., Francis, J., Le Boeuf, B. J., Horning, M., Calambokidis, J. and Croll, D. A. (2000). Sink or swim: strategies for cost efficient diving by marine mammals. *Science* **288**, 133-136.
Williams, T. M., Fuiman, L. A., Horning, M. and Davis, R. W. (2004). The cost of foraging by a marine predator, the Weddell seal *Leptonychotes weddellii*: pricing by the stroke. *J. Exp. Biol.* **207**, 973-982.
Williams, T. M., Noren, S. R. and Glenn, M. (2011). Extreme physiological adaptations as predictors of climate-change sensitivity in the narwhal, *Monodon monoceros*. *Mar. Mamm. Sci.* **27**, 334-349.